

## Universal Temperature Dependence, Flux Extinction, and the Role of $^3\text{He}$ Impurities in Superfluid Mass Transport through Solid $^4\text{He}$

Ye. Vekhov, W. J. Mullin, and R. B. Hallock

*Laboratory for Low Temperature Physics, Department of Physics, University of Massachusetts, Amherst, Massachusetts 01003, USA*  
(Received 14 April 2014; revised manuscript received 10 June 2014; published 17 July 2014)

The mass flux,  $F$ , carried by as-grown solid  $^4\text{He}$  in the range 25.6–26.3 bar rises with falling temperature, and at a concentration-dependent temperature,  $T_d$ , the flux decreases sharply within a few mK. We study  $F$  as a function of  $^3\text{He}$  impurity concentration,  $\chi$ . We find that  $T_d$  is an increasing function of increasing  $\chi$ . At temperatures above  $T_d$  the flux has a universal temperature dependence and the flux terminates in a narrow window near a characteristic temperature  $T_h \approx 625$  mK, which is independent of  $\chi$ .

DOI: 10.1103/PhysRevLett.113.035302

PACS numbers: 67.80.bd, 71.10.Pm

The torsional oscillator measurements on solid  $^4\text{He}$  by Kim and Chan [1,2] stimulated substantial interest in the properties of solid  $^4\text{He}$ . Changes in the stiffness [3] of  $^4\text{He}$  were found to have a temperature dependence very similar to the period shifts seen in the torsional oscillator work. More recent work by Chan's group that utilized a Vycor cell coated with epoxy (that contained no bulk solid  $^4\text{He}$ ) showed no significant period shifts [4]. It is now believed by many that the original Kim and Chan [1,2] observations resulted from changes in the stiffness [3] of the bulk helium in the sample cell and the influence of this temperature-dependent stiffness on the torsional oscillator itself and not from supersolidity.

Experiments designed to create mass flow in solid  $^4\text{He}$  in confined geometries by directly squeezing the solid lattice have not been successful [5–8]. But, by the creation of chemical potential differences across bulk solid samples in contact with superfluid helium, a mass flux,  $F$ , has been documented [9,10]. For  $^4\text{He}$  with a nominal 0.3 ppm  $^3\text{He}$  content those experiments revealed the strong temperature dependence [11,12] of  $F$  at  $T_d \approx 75$ –80 mK, with behavior at higher temperatures that indicated the presence of a bosonic Luttinger liquid [13–15]. The details of what is definitively responsible for this have not been established. The results to date are consistent with dissipative superflow along one-dimensional dislocation cores [16], but alternate scenarios have been suggested [17]. In the present work we report measurements of  $F$  and  $T_d$ , as a function of  $^3\text{He}$  impurity concentration,  $\chi$ , in the pressure range 25.6–26.3 bar and conclude that the extinction of the flux at  $T_d$  is related to  $^3\text{He}$  leaving the solid mixture and blocking the flux carriers. For  $T > T_d$  the flux is sample dependent, has a universal temperature dependence, and terminates in a narrow window near a characteristic temperature  $T_h \approx 625$  mK, which is independent of  $\chi$ . Cooling through  $T_d$  the flux drops sharply within a few mK.

Since the apparatus [11,12] used for this work has been illustrated and described in detail previously, our description here will be very brief. Solid helium in an experimental

cell is penetrated on two sides by superfluid-filled Vycor rods V1 and V2, which in turn are in contact with separate reservoirs R1 and R2 filled with superfluid. During the experiments, a temperature gradient is present across the superfluid-filled Vycor [18–20] rods, which ensures that the reservoirs remain filled with superfluid, while the solid-filled cell remains at a low temperature. For the present experiments an initial chemical potential difference,  $\Delta\mu_0$ , can be imposed by the creation of a temperature difference,  $\Delta T = |T1 - T2|$ , between the reservoirs. The result is a mass flux through the solid between the Vycor rods, and a change in the fountain pressure between the two reservoirs to restore equilibrium.

To fill the cell initially, helium gas, typically assumed to contain  $\sim 0.3$  ppm  $^3\text{He}$ , but for this work measured to be 0.17 ppm  $^3\text{He}$ , is condensed through a direct-access heat-sunk capillary, which enters the cell at its midpoint. To grow a solid at constant temperature from the superfluid, which is our standard technique, we begin with the pressure in the cell just below the bulk melting pressure for  $^4\text{He}$  at the growth temperature (typically  $\sim 300$ –400 mK) and then add atoms simultaneously through capillaries that enter the separate reservoirs. As with many experiments with solid  $^4\text{He}$ , we have no direct knowledge of the sample crystal quality, but presume that it has substantial sample-dependent disorder, unless annealed.

To study the effect of the  $^3\text{He}$  impurities the cell is emptied between each sample and a new concentration is introduced. To accomplish this, the cell is again filled with  $^4\text{He}$  liquid (0.17 ppm  $^3\text{He}$ ). Then a small calibrated volume at room temperature is filled with pure  $^3\text{He}$  to a known pressure. This is injected into the cell via the same direct-access capillary and is followed by additional  $^4\text{He}$ , which also enters through the capillary, to bring the cell to the melting curve. With knowledge of the relevant volumes and pressures, a concentration of  $^3\text{He}$  is thus introduced into the cell. A solid is created (with the direct-access capillary closed) by further additions of  $^4\text{He}$  by use of the capillary lines that enter each reservoir, the sample solidifies, and

additional  $^4\text{He}$  is added to bring the pressure of the hcp solid to the desired range. The solid is then allowed to equilibrate, typically for several hours at  $T \leq 0.4$  K.

With stable solid  $^4\text{He}$  in the cell, we use heaters  $H1$  ( $H2$ ) to change the reservoir temperatures  $T1$  ( $T2$ ) to create an initial chemical potential difference,  $\Delta\mu_0$ , between the reservoirs and then measure the resulting changes [21] in the reservoir pressures  $P1$  and  $P2$ . This allows us to determine the time dependence of the chemical potential difference,  $\Delta\mu$ , that drives the flux [13]. We take  $F = d(P1 - P2)/dt$  (here consistently measured at  $\Delta\mu = 5$  mJ/g) to be proportional to the flux of atoms that passes through the solid. We report our flux values in mbar/s, where a typical value of 0.1 mbar/s corresponds to a mass flux through the cell of  $\approx 4.8 \times 10^{-8}$  g/s.

Examples of the temperature dependence of the flux are shown in Fig. 1 for a number of different samples and values of  $\chi$ . We document an abrupt  $\chi$ -dependent reduction of the flux at a characteristic temperature,  $T_d$ . Our present measurements for a  $\chi = 0.17$  ppm sample confirm the decrease in the flux in the vicinity of 75–80 mK that was seen previously for nominal 0.3 ppm  $^3\text{He}$  [11,12]. We also confirm that near the foot of the drop in flux for  $\chi < 5$  ppm the flux can be rather unstable in time and after falling in a narrow temperature range can sometimes be nonzero and increase with a further decrease in temperature. Figure 2 illustrates how sharp the flux extinction can be. In this  $\chi = 10$  ppm  $^3\text{He}$  example there is robust flux for the solid at 102.6 mK and also at 101.1 mK, but at the temperature of 99.8 mK the flux has been extinguished. This is evident 300 seconds after the change in cell temperature to 99.8 mK, when the reversal of the applied  $\Delta\mu_0$  produces no measurable flux. An increase in the temperature of  $\approx 1$  mK results in an accelerating recovery of the flux to the previous value, Fig. 3, with a time for recovery of  $\approx 500$  sec. We also note, Fig. 1, that some

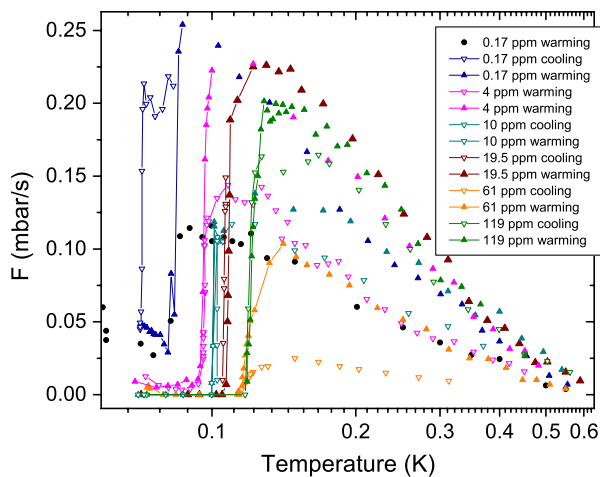


FIG. 1 (color online). The temperature dependence of the sample-dependent flux for various concentrations. Lines are guides to the eye.

hysteresis is present at  $T_d$  and that increasing concentrations of  $^3\text{He}$  appear to cause a change in the  $T_d$  flux extinction to a somewhat less precipitous behavior.

The addition of  $^3\text{He}$  has no measurable effect on the nonhysteretic temperature dependence of the flux for  $T > T_d$ . Different freshly made samples typically provide different flux values. Samples that are warmed to 500–650 mK or above (where the flux gets unstable or falls to zero) can show significantly lower flux when cooled—in some cases showing no flux. Samples annealed near 1 K for  $\sim 10$  h show no flux when cooled and pressure gradients that existed when the sample was grown are removed. After cooling, low (or zero) flux values can typically be increased by changing the pressure in the cell. In all cases of nonzero flux, normalization of the data sets at 200 mK shows that they all have the same universal-like temperature dependence as illustrated in Fig. 4. All of the data suggest that at higher temperature the behavior of the flux extrapolates to zero near  $T_h \approx 625$  mK, a value consistent within errors with earlier measurements [11,12] with nominal 0.3 ppm samples.

In Fig. 5 we illustrate the measured  $T_d$  vs  $\chi$ . The general trend of these  $T_d$  vs  $\chi$  data is reminiscent of a phase separation curve. With this in mind, also shown on Fig. 5 are the results of calculations of homogeneous phase separation. As a first approximation, the coordinates of homogeneous phase separation for the solid-solid ( $^4\text{He}$ -rich hcp- $^3\text{He}$ -rich bcc; dashed line) case are obtained by use of the prescription described by Edwards and Balibar [22]:  $T_p^s = [(0.80)(1-2\chi) + 0.135]/\ln(1/\chi-1)$ . In our case, this prescription needs modification since at our pressure of 25.8 bar if the  $^3\text{He}$  separates into macroscopic regions we expect that it to be liquid [23–25]. We have recalculated

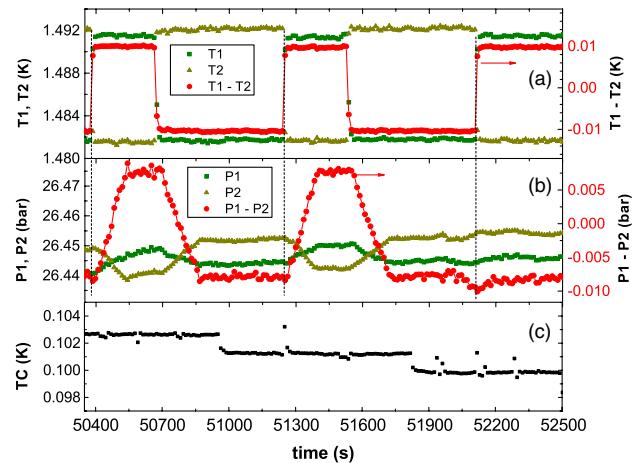


FIG. 2 (color online). An example of the sharpness of the extinction of the flux for  $\chi = 10$  ppm. (a) The reservoir temperatures are reversed to initiate flow in one direction or the other:  $\Delta T = T1 - T2$ . (b) The resulting pressure changes allow a measurement of the  $F$ :  $\Delta P = P1 - P2$ . (c) The cell temperature is reduced in a stepwise fashion.

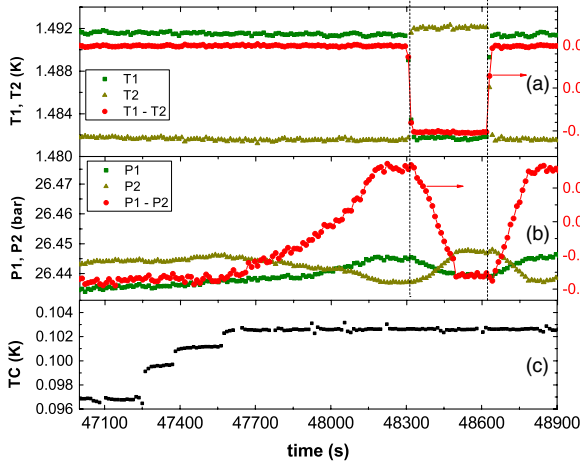


FIG. 3 (color online). Similar to the previous figure. Here in spite of an imposed  $\Delta T$ , no flow results until  $T$  exceeds  $T_d$ , after which the kinetics of the rising flux are visible.

homogeneous phase separation for the solid-liquid ( $^4\text{He}$ -rich hcp- $^3\text{He}$ -rich liquid) case using the prescription of Edwards and Balibar [22] for evaluating the necessary parameters at our pressure and the corresponding  $T_p^s$ , Fig. 5 (solid line). There is limited experimental data in the literature on solid phase separation in our experimental regime [25].

The fact that an increase in concentration shifts  $T_d$  to higher values motivates a scenario for the role of the  $^3\text{He}$  in these experiments. We noted above that the 10 ppm sample, given a 1 mK decrease in cell temperature to 99.8 mK followed by a wait of 300 s, produced no flux following the reversal of  $\Delta\mu_0$ . Indeed there is evidence in the data that the transition from flow to no flow takes place within  $\sim 150$  seconds. Given that the time required for a complete phase separation transition in solid mixture solutions is typically measured in hours [23–25], e.g.,  $\sim 10$  h, the disparity between these two times is striking. This suggests that only a small amount of the  $^3\text{He}$  needs to be involved to extinguish the flux.

Since solid helium has demonstrated one-dimensional bosonic Luttinger liquid behavior [13], we consider the possibility that dislocation cores and their intersections are responsible for the flux and these are blocked by the  $^3\text{He}$ . It is predicted that the addition of  $^3\text{He}$  along a dislocation core will diminish the superfluid density there [26], particularly where such cores intersect. Given the number of  $^3\text{He}$  available and the likely number ( $\sim 10^5$ ) of such structures that provide the conducting pathways between the Vycor rods [13], there is more than enough  $^3\text{He}$  to quickly provide for the extinction of the flux. It is enough that a short segment or intersection along the Vycor-to-Vycor pathway that spans the cell be decorated and this should take place relatively quickly.

The inset to Fig. 5 shows  $\ln(\chi)$  vs  $1/T$ . At small  $\chi$  the bulk phase separations satisfy  $\chi = \exp(-R/T)$  with  $R$

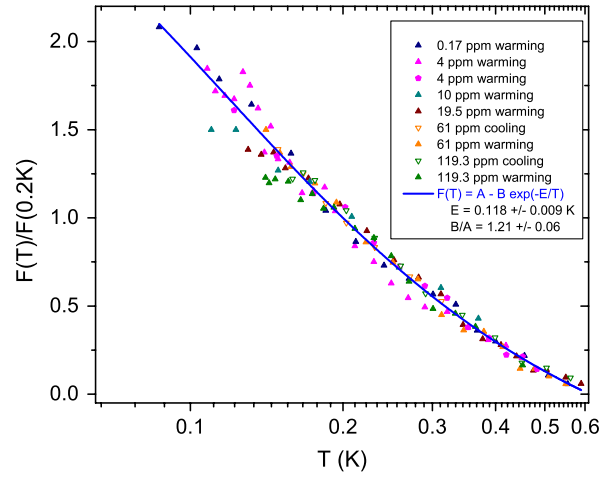


FIG. 4 (color online). The temperature dependence of the normalized flux observed for  $^4\text{He}$  with several  $^3\text{He}$  impurity concentrations and experimental conditions for  $T > T_d$ . Fitted line: see text.

approximately independent of temperature, and  $R = 0.94$  K and  $1.02$  K for solid-solid and solid-liquid bulk phase separation, respectively. A fit of the data (red circles, black solid line) by  $\chi = \exp(-R/T)$  yields  $R = 1.17$  K. A model that includes a small number of binding sites for  $^3\text{He}$  or  $^4\text{He}$  atoms yields the functional form  $\chi = \exp(a - R/T)$ , where  $\exp(a)/(1 + \exp(a))$  is the minimum concentration that blocks superflow, and  $R$  includes the binding energy. With this functional form, we find a much better fit (solid red line), with  $R = 1.48$  K and  $a = 3.36$ . This energy value is higher than the predicted [26,27] binding energy ( $\sim 0.7$  K) of single  $^3\text{He}$  atoms to dislocation cores. This supports the possibility that the flux extinction results from the  $^3\text{He}$  binding to dislocation intersections [26], where the  $^3\text{He}$  blocks the flux.

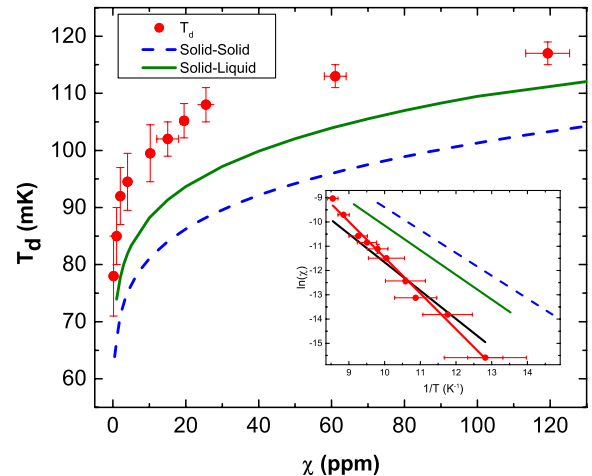


FIG. 5 (color online). Temperature of the sharp drop in  $F$ ,  $T_d$ . Inset:  $\ln(\chi)$  vs  $1/T$ ; see text.

The robust nonhysteretic and universal temperature dependence for temperatures between  $T_d$  and near but below  $T_h$  suggests to us the following scenario. A given sample preparation results in a given number of structures that span the sample between the Vycor rods and carry the flux. We believe that an increase in temperature reduces the effective conductivity of the structures (which includes their connection to the superfluid-filled Vycor) that carry the flux. From this perspective conducting pathways remain robust until a high enough temperature is reached at which some (or all) of the pathways are somehow irreversibly interrupted. Indeed, as we have noted, it can be the case that an increase in the temperature of the solid well above  $T_h$  leads to no flux when the cell is cooled. This no-flux situation can be changed by an imposed change in the amount of  $^4\text{He}$  in the cell, which apparently introduces structural changes, which create new pathways for the flux. In this scenario all of the temperature dependence well above  $T_d$  is dictated by changes in conductivity along the existing pathways.

To follow this line of thought, suppose an activated process exists that degrades the flux with increasing efficiency according to  $\sim \exp(-E/T)$ . For example, thermally activated jogs or kinks [28] (roughness) on dislocation cores would introduce disorder and phase slips would result. It is reasonable to assume that the flux might obey a form such as  $F = A - B \exp(-E/T)$ . We have applied this to the data shown in Fig. 4 and we find that  $B/A = 1.21 \pm 0.06$  and thus the data can be well fit with the form  $F/F(0.2K) = F_0[1 - 1.21 \exp(-E/T)]$ , with  $E = 118 \pm 9$  mK, Fig. 4. In this scenario, when  $F = F_0^*[1 - 1.21 \exp(-E/T)]$  is applied to non-normalized individual data sets,  $F_0^*$  should in each case be proportional to the number of conducting pathways between the Vycor rods.

In summary, we find that the addition of  $^3\text{He}$  to concentrations above the nominal  $\chi$  found naturally in well helium serves to increase the temperature at which a sharp drop in flux through the solid-filled sample cell takes place. We find that the temperature dependence of the flux at higher temperatures is universal and the flux terminates in a narrow window near a characteristic temperature  $T_h \approx 625$  mK. These measurements impose constraints that any explanation of the flux must satisfy and support the possibility that the flux is carried by dislocation cores and is blocked by  $^3\text{He}$  binding.

We thank B. V. Svistunov, N. V. Prokof'ev, and A. B. Kuklov for a number of stimulating discussions, N. S. Sullivan and D. Candela for comments on phase separation, and M. W. Ray for early work on the apparatus. This work was supported by NSF Grants No. DMR 12-05217 and No. DMR 08-55954 and by University Research Trust Funds.

- [1] E. Kim and M. Chan, *Nature (London)* **427**, 225 (2004).
- [2] E. Kim and M. Chan, *Science* **305**, 1941 (2004).
- [3] J. Day and J. Beamish, *Nature (London)* **450**, 853 (2007).
- [4] D. Y. Kim and M. H. W. Chan, *Phys. Rev. Lett.* **109**, 155301 (2012).
- [5] D. S. Greywall, *Phys. Rev. B* **16**, 1291 (1977).
- [6] J. Day, T. Herman, and J. Beamish, *Phys. Rev. Lett.*, **95**, 035301 (2005).
- [7] J. Day and J. Beamish, *Phys. Rev. Lett.* **96**, 105304 (2006).
- [8] A. C. Rittner, W. Choi, E. J. Mueller, and J. D. Reppy, *Phys. Rev. B*, **80**, 224516 (2009).
- [9] M. W. Ray and R. B. Hallock, *Phys. Rev. Lett.* **100**, 235301 (2008).
- [10] M. W. Ray and R. B. Hallock, *Phys. Rev. B* **79**, 224302 (2009).
- [11] M. W. Ray and R. B. Hallock, *Phys. Rev. Lett.* **105**, 145301 (2010).
- [12] M. W. Ray and R. B. Hallock, *Phys. Rev. B* **84**, 144512 (2011).
- [13] Y. Vekhov and R. B. Hallock, *Phys. Rev. Lett.* **109**, 045303 (2012).
- [14] A. Del Maestro and I. Affleck, *Phys. Rev. B* **82**, 060515(R) (2010).
- [15] A. Del Maestro, M. Boninsegni, and I. Affleck, *Phys. Rev. Lett.* **106**, 105303 (2011).
- [16] Ş. G. Söyler, A. B. Kuklov, L. Pollet, N. V. Prokof'ev, and B. V. Svistunov, *Phys. Rev. Lett.* **103**, 175301 (2009).
- [17] S. Sasaki, F. Caupin, and S. Balibar, *J. Low Temp. Phys.* **153**, 43 (2008).
- [18] J. R. Beamish, A. Hikata, L. Tell, and C. Elbaum, *Phys. Rev. Lett.* **50**, 425 (1983).
- [19] C. Lie-zhao, D. F. Brewer, C. Girit, E. N. Smith, and J. D. Reppy, *Phys. Rev. B* **33**, 106 (1986).
- [20] E. Adams, Y. Tang, K. Uhlig, and G. Haas, *J. Low Temp. Phys.* **66**, 85 (1987).
- [21] M. W. Ray and R. B. Hallock, *Phys. Rev. B* **82**, 012502 (2010).
- [22] D. O. Edwards and S. Balibar, *Phys. Rev. B* **39**, 4083 (1989).
- [23] A. N. Gan'shin, V. N. Grigor'ev, V. A. Maidanov, N. F. Omelaenko, A. A. Penzev, E. Y. Rudavskii, A. S. Rybalko, and Y. A. Tokar, *Low Temp. Phys.* **25**, 592 (1999).
- [24] C. Huan, S. Kim, L. Yin, J. Xia, D. Candela, and N. Sullivan, *J. Low Temp. Phys.* **162**, 167 (2011).
- [25] S. S. Kim, C. Huan, L. Yin, J. Xia, D. Candela, and N. S. Sullivan, *Phys. Rev. Lett.* **106**, 185303 (2011).
- [26] P. Corboz, L. Pollet, N. V. Prokof'ev, and M. Troyer, *Phys. Rev. Lett.* **101**, 155302 (2008).
- [27] O. Syshchenko, J. Day, and J. Beamish, *Phys. Rev. Lett.* **104**, 195301 (2010).
- [28] D. Aleinikava and A. Kuklov, *J. Low Temp. Phys.* **169**, 133 (2012).